CrossMark

ORIGINAL PAPER

TEMPO-oxidized cellulose nanofibers as potential Cu(II) adsorbent for wastewater treatment

Núria Fiol · Matías G. Vásquez · Miguel Pereira · Quim Tarrés · **Pere Mutjé · Marc Delgado-Aguilar**

Abstract Cellulose nanofibers (CNFs) are becoming a topic of great interest due to their wide range of potential applications. The huge presence of carboxylic groups in TEMPO-oxidized CNFs indicate that this material could interact with cationic species in aqueous solution, such as metal ions. Nevertheless, the contact between nanofibers and water solutions requires a 3D structure to entrap and retain the nanofibers. In this sense, two different 3D structures were synthetized: CNF-calcium alginate beads and CNF-aerogels. After the synthesis and characterization of 3D structures, batch sorption studies were performed by using these sorbents to study their ability for metal removal. Equilibrium data fitted very well Langmuir and Freundlich isotherm models in the studied concentration range of copper(II) ions and confirmed that the copper sorption is a favorable process. Both new synthetized materials resulted to be effective for Cu(II) removal and maximum sorption capacity was higher for CNF-aerogels than CNF-calcium alginate beads. Finally, in this work it has been demonstrated that the synthetized 3D CNF-aerogel structure is an efficient sorbent for copper ion removal from aqueous solutions and the use of this synthetized structure for environmental decontamination opens a new opportunity to CNF applications.

N. Fiol
Chemical Engineering Department, University of Girona, C/Maria Aurèlia Capmany, 61, 17003 Girona, Spain

M. G. Vásquez
Faculty of Forestry Sciences, University of Concepción, Casilla 160-C Concepción, Chile

M. Pereira
Departamento de Ingeniería Química, Facultad de Ingeniería, Universidad de Concepción, Casilla 160-C Concepción, Chile

Q. Tarrés (✉) · P. Mutjé · M. Delgado-Aguilar
LEPAMAP Research Group, Chemical Engineering Department, University of Girona, C/Maria Aurèlia Capmany, 61, 17003 Girona, Spain
e-mail: joaquimagusti.tarres@udg.edu

Graphical abstract

CNF/Alginate treatment up to 60% Cu removal
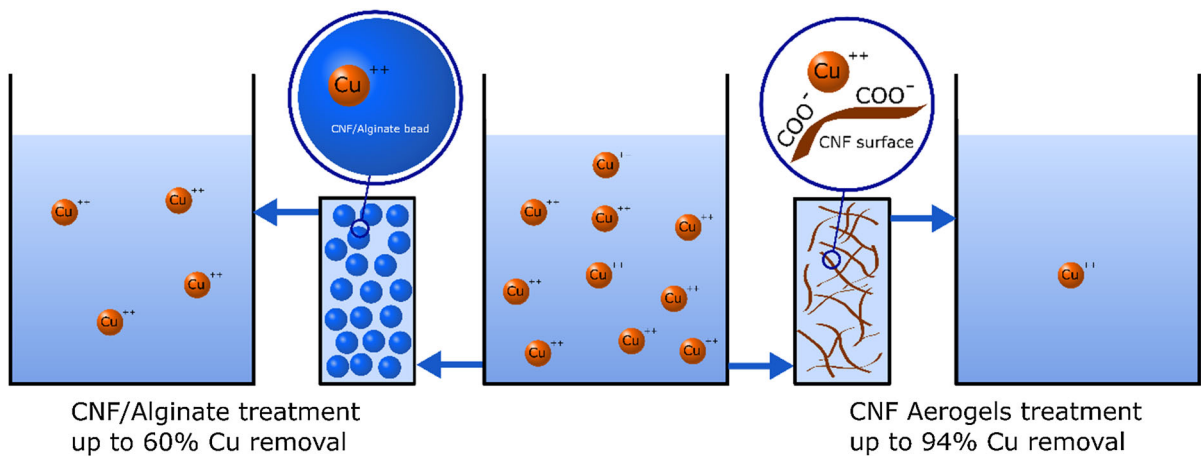
CNF Aerogels treatment up to 94% Cu removal

Introduction

Water is indispensable for life and our planet is endowed with water and the necessary elements to support such life. However, out of all the water on Earth, about 97% corresponds to oceans, seas and saline groundwater. In this sense, only 2.5–2.75% is fresh water, which includes 1.75–2% of frozen water in glaciers, ice and snow. Overall, only 0.5–0.75% of water is fresh groundwater and soil moisture, and less than 0.01% can be found in lakes, swamps and rivers. Out of this 0.01%, 34% can be found in Africa, 26% in Russia, 25% in North America and the 15% remaining in other lakes randomly distributed across the Earth's surface in small lakes and rivers (Pidwirny 2006; USGS 2013).

Considering the rapid growing rate of the global population, the improvements on their living standards and, consequently, the increase on industrial operations, the higher demand of water resources and generation of wastewater is understandable (Batmaz et al. 2014). With the increasing generation of wastewater, the concentration of heavy metals in rivers can be dramatically increased, derived from industrial, mining and/or agricultural activities. Such heavy metals, at high concentrations, can be toxic for animals and humans, leading to serious health

complications, causing even death in extreme cases. The removal of such metals is not only interesting to prevent such diseases, but also to reuse them in several industrial applications (Glover-Kerkvliet 1995; Hokkanen et al. 2013). There is a wide range of methodologies to remove heavy metals from wastewater, such as reverse osmosis, precipitation, ion exchange based systems or even micro and nanofiltration. However, most of the abovementioned processes are energy consuming and some of them require the use of other chemicals such as anionic flocculants with high cationic demand. Ion exchange based systems based on the adsorption of heavy metal ion retention at the surface of modified adsorbents is a good strategy and has been investigated by many researchers (Wan Ngah and Hanafiah 2008; Vinícius et al. 2009). However, in some cases they are not cost-effective and require the use of non-renewable materials and also organic solvents (Batmaz et al. 2014).

In the recent years, cellulose nanofibers (CNFs) are becoming a topic of great interest due to the wide range of applications they can be used in, such as paper reinforcement and coating (Hii et al. 2012; Tarrés et al. 2018), films made thereof called nanopapers (Sehaqui et al. 2010; Tarrés et al. 2017), biomedicine (Lin and Dufresne 2014), electronics (Lay et al. 2016; Lizundia et al. 2016) and environmental (Zhang et al. 2014), among others. In addition, CNFs are also attractive because it is based on renewable and abundant resources that can be processed with well-established pulp, paper and wood industry methods. Among all the methods to produce CNFs, TEMPO-mediated

oxidation has become broadly popular, at least at laboratory scale, during the recent years. Basically, the reaction consists on selectively oxidizing the C6 of the D-glucose unit by substituting the –OH group of the carbon by a COOH or COONa group, depending on the pH (Saito et al. 2007). The reaction can be conducted either with NaClO or NaClO$_2$ as oxidizers in presence of NaBr at alkaline or neutral conditions and the catalyst is 2,2,6,6-tetramethylpiperidine-1-oxyl radical (TEMPO), which is water soluble, commercially available and has a negative result for the Ames test (Isogai et al. 2011). Although TEMPO-mediated oxidation has been considered as an expensive treatment, making unfeasible its upscaling, in a recent work it was shown that production costs could be significantly decreased by means of optimizing the amount of catalyst and, on the other hand, using industrial reagents (Batmaz et al. 2014; Serra et al. 2017).

TEMPO-oxidized CNFs present a huge specific surface which, depending on the treatment severity, can range from 150 to 350 m^2/g. This specific surface promotes the availability of COO$^-$ groups, either in their acid or salt form. In fact, the strategy of introducing carboxyl groups onto cellulose surface has been previously studied, but in all cases a post-production surface modification was required (Low et al. 2004; Alves-Gurgel et al. 2008; Hokkanen et al. 2013; Batmaz et al. 2014). Due to the huge hydrophilic character of CNFs, their use in wastewater requires their assembling in dried 3D-structured networks. In this sense, the development of CNF-based aerogels has been reported to be an effective method to preserve their huge specific surface while they can be manipulated in water-based systems (Tarrés et al. 2016). In addition, the use of such structures can be advantageous in terms of recovering the saturated material. This approach has been previously tackled, but some other polymers were required for metal ion recovery or, otherwise, chemical modifications were conducted to the cellulose nanofibers surface, leading to sophisticated methodologies (Maatar and Boufi 2015; Mahfoudhi and Boufi 2017). Another approach can be the development of encapsulating systems, such is the case of calcium alginate beads, which has been previously successfully used as entrapped gel matrix for micro and nanoparticles to form homogeneous and permeable spheres (Fiol et al. 2004; Bezbaruah et al. 2009).

For all the above, the present work aims at developing hybrid structures based on alginate and CNFs to remove Cu(II) from different solutions, as well as exploring the use of porous structures based on CNFs. For this, alginate beads containing from 0 to 0.8 wt% of CNFs were prepared and submitted to batch experiments in 15, 100 and 1000 mg/L Cu(II) solutions. The same process was repeated with CNF-based aerogels. Finally, the present work studies the adsorption mechanisms through Langmuir and Freundlich isotherms.

Materials and methods

Cellulose nanofibers production and characterization

Bleached kraft eucalyptus pulp was kindly provided by ENCE Celulosa y Energía S.A. (Spain) and was used as raw material for CNFs production. The oxidation degree of CNFs was set at 25 mmols/g of fiber. In a typical experiment, 15 g of fiber were dispersed in distilled water containing TEMPO (0.016 g per g of fiber) and NaBr (0.1 g per g of fiber). The mixture was stirred for 15 min in order to assure good dispersion of all the substances. Then, the desired amount of NaClO was added drop-wise to the pulp slurry keeping the pH at 10. Once all the NaClO was added, the pH was further kept at 10 by means of NaOH addition until no pH variation was observed. The oxidized fibers were then filtered and washed with distilled water. Then, 1% de fiber suspensions were gradually homogenized in a PANDA Plus laboratory homogenizer (Gea Niro Soavi, Italy) following the sequence of 3 passes at 300 bar and 3 passes at 600 bar. The homogenized suspension were stored in plastic bottles at 4 °C for further use. All the reagents required for the oxidation were acquired from Sigma Aldrich (Spain) and were used as received.

Yield of fibrillation was determined by centrifuging a 0.2 wt% suspension at 4500 rpm for 20 min in order to isolate the nanofibrillated fraction (contained in the supernatant) from the non-fibrillated and partially fibrillated one, retained in the sediment fraction. The supernatant was then removed from the container and the sediment was oven-dried at 105 °C until constant weight. The yield of fibrillation was then calculated using the equation:

$$Yield(\%) = \left(1 - \frac{\textit{weight of dried sediment}}{\textit{weight of diluted sample}} \cdot \%Sc\right) \times 100$$

(1)

where %Sc is the solid content of the diluted CNF sample.

The degree of polymerization (DP) was determined from intrinsic viscosity measurements, according to UNE 57-039-92. The viscosimetric average molecular weight was calculated from the equation:

$$\eta = K \cdot M^a$$

(2)

where η is the intrinsic viscosity (dL/g), K and a are constants (2.28 and 0.76 respectively), which depend on the polymer–solvent system; and M is the molecular weight (Henriksson et al. 2007).

The water retention value (WRV) was calculated by separating a given volume of CNF gel into 2 identical portions, which were then centrifuged in a Sigma Laborzentrifugen model 6K15 (SIGMA, Germany) at 2400 rpm for 30 min to eliminate non-bonded water. The suspension was filtered through nitrocellulose membrane with a pore size of 0.22 μm diameter set at the bottom of the centrifuge bottles. After centrifugation, only the CNFs in contact with the membrane were recovered, weighted and the dried at 105 °C for 24 h in previously weighed bottles. The average WRV was finally calculated according to the equation:

$$WRV(\%) = \left(\frac{W_w - W_d}{W_d}\right) \cdot 100$$

(3)

where W_w is the wet weight (g), W_d the dry weight (g).

Carboxyl content (CC) was used to monitor the effectiveness of the TEMPO-mediated oxidation of the fibers and it was determined by means of conductimetric titration, as it has been previously reported (Besbes et al. 2011). The dried sample (30–40 mg) was suspended in 15 mL of 0.01 M HCl, exchanging Na$^+$ cations (bonded to the COO$^-$ groups) by H$^+$ protons. Then, the suspension was titrated with a 0.01 M NaOH solution, recording the conductivity every 0.1 mL of NaOH added. Typical conductimetric curves experience a reduction, stabilization and increase in conductivity. In this sense, NaOH was added until this pattern was observed. The curve exhibited the presence of a strong acid, corresponding to the excess of HCl and a weak acid, which can be attributed to the carboxylic acid at the surface of cellulose chains. Thus, the CC is given by Eq. 4.

$$CC = 162 \cdot (V_2 - V_1) \cdot c \cdot [w - 36 \cdot (V_2 - V_1) \cdot c]^{-1}$$

(4)

where V_2 and V_1 are the equivalent volumes of the added NaOH solution (L) during the increase and decrease on conductivity, respectively, w is the dry weight of the sample (g) and c is the NaOH concentration (mol/L).

Cationic demand of the LCMNF suspension, understood as the amount of standard cationic polymer required to neutralize the highly anionic surface of the LCMNF, was measured by means of a Mütek PCD 04 particle charge detector from BTG International Ltd (United Kingdom). First of all, LCMNF were dispersed in a poly-DADMAC solution at 0.1 wt% and stirred for 10 min. Then, the suspension was centrifuged to promote LCMNF precipitation. The supernatant was then titrated with the anionic standard polymer Pes-Na. Both standard polymers were acquired from BTG.

Specific surface and diameter were estimated from cationic demand and carboxyl content, as described by Espinosa et al. (2016). Briefly, it was considered that the interaction between the CNF surface and the added cationic polymer (poly-DADMAC) occurred through two different mechanisms: on the one hand, part of the polymer got retained by ionic interaction between carboxylic groups from CNFs and the polymer thereof. On the other, the rest of the consumed poly-DADMAC during cationic demand determination was assumed to be retained by hydrogen bonding and Van der Waals forces. This can be assumed due to the high molecular weight of the poly-DADMAC that was used. Indeed, low-MW polymers could penetrate into the cellulose fiber cell walls, while high-MW polymers cannot (Lizundia et al. 2016).

Moreover, the estimation of the specific surface was accomplished taking into account two assuptions: (i) the surface adsorption of poly-DADMAC took place in the form of a monolayer and (ii) the poly-DADMAC chain has a cylindrical geometry. The surface of poly-DADMAC was initially estimated by calculating the surface of the monomer and its polymerization degree, taking into account the bond distances and assuming a cylindrical monomer

$(535.87 \text{ nm}^2/\text{g}$, being equal to $4.87 \times 10^{17} \text{ nm}^2/\mu\text{eq}\cdot\text{g})$.

Moreover, using the values obtained for cationic demand and the carboxyl content it was possible to calculate the CNF theoretical surface area by the following equation:

$$\sigma_{CNF} = (CD - CC) \cdot S_{Poly\{-\}DADMAC} \quad (5)$$

where CD is cationic demand, CC is carboxyl content (both expressed in $\mu\text{eq}\cdot\text{g/g}$) and $S_{Poly\text{-}DADMAC}$ is the specific surface of Poly-DADMAC, in $\text{nm}^2/\mu\text{eq}\cdot\text{g}$.

Finally, assuming that nanofibers are perfect cylinders and that cellulose density is 1.5 g/cm^3, diameter was estimated.

Transmittance measurements of the CNF suspension was performed on a 0.1 wt% suspension using quarz cuvettes and a UV–Vis Shimadzu spectrophotometer UV-160A set in the range between 400 and 800 nm. Distilled water was used as reference and background.

Preparation of the CNF/Alginate beads

For the formation of the CNF/Alginate beads, three different CNF consistencies were used: 0.2, 0.5 and 0.8 wt%. In a typical experiment, 25 mL of CNF suspension was mixed with 25 mL of sodium alginate 1 wt% solution and kept under gentle stirring. The resulting suspension was pumped by means of a peristaltic pump working at continuous flow and equipped with a micropipette tip at the outlet. The droplets were collected in a stirred tank containing 100 mL of 0.5 M CaCl$_2$ solution. Due to ionic exchange between Na$^+$ and Ca^{2+} cations, beads were formed when both solutions got in contact. The formed beads were kept under stirring in the CaCl$_2$ solution for 24 h to ensure a proper hardening. Then, the beads were filtered and rinsed several times with distilled water to remove the excess of calcium chloride from their surface. This process was carried out four times in so far as obtaining the reference (without CNFs) and beads with the 0.2, 0.5 and 0.8 wt% CNF solution. The whole process can be observed in Fig. 1.

Physical characterization of the CNF/Alginate beads

The obtained beads were characterized in terms of morphology, density and water content. Water content was measured by means of gravimetric methods: 40 beads were suspended in water for 24 h and then filtered until no dewatering was observed. The beads were weighted and then dried in an oven at 105 °C until constant weight. The dried beads were weighted again. This methodology provided the amount of water per dry gram of CNF/Alginate, as well as the amount of water per bead. Average bead diameter was determined by measuring the diameter of 40 beads with a Vernier caliper with a resolution of 0.1 mm. Density of wet beads was determined by dividing the wet weight by the average volume of the beads.

Preparation of CNF-based aerogels

CNF suspensions at 0.5 wt% consistency were poured into metallic dishes and frozen at − 80 °C for 3 h. Then, the frozen suspensions were freeze-dried in a lyophilizer until constant weight. Finally, the aerogels were milled to be distributed in the batch. Aerogels were observed through field-emission scanning electron microscopy using a Hitachi S-3000 (Spain) microscope, working at 12 kV; samples were previously covered with carbon via sputtering.

Batch Cu(II) uptake procedure

Batch experiments were conducted at 20 ± 1 °C in stoppered glass tubes containing 15 mL of different aqueous Cu(II) solutions. The tubes were shaken at 25 rpm in a rotary mixer (Cenco Instrument) for 1 h. Then, the beads were filtered through a 0.45 μm cellulose filter paper (Millipore) and solution pH was measured. Initial and final copper concentration in the filtrates before and after sorption, previously acidified, were determined by Flame Atomic Absorption Spectrometry (FAAS) in a Varian Absorption Spectrometer SpectrAA 220FS. The copper concentration in the solid phase was obtained from the difference between initial and final metal concentration in the solution. Thus, the relative amount of copper that was removed was calculated according to Eq. 6.
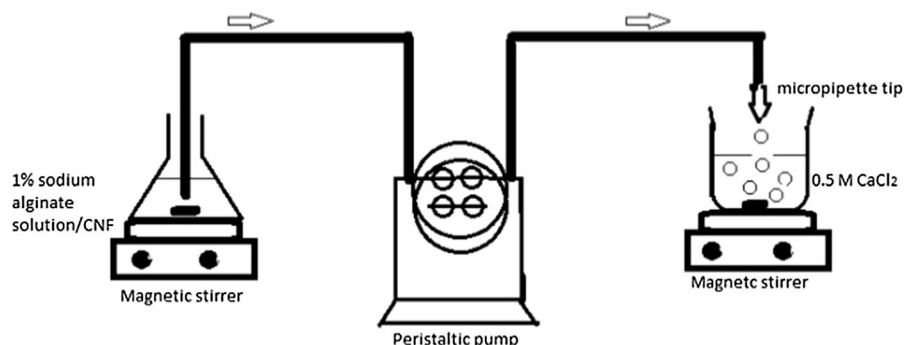
Fig. 1 Schematic preparation process of the CNF/Alginate beads

$$\%R = \frac{C_i - C_{eq}}{C_i} \cdot 100 \qquad (6)$$

where C_i and C_{eq} are the initial and final equilibrium metal concentration in solution, respectively.

The experiments were carried out at three different Cu(II) solution concentrations (15 mg/L, 0.1 g/L and 1.0 g/L) over alginate beads containing 0.0, 0.2, 0.5 and 0.8 wt% of CNFs and also over CNF aerogel with 0.5, 1.0 and 2.0 wt% of AKD. In the case of beads, the amount was set to 35 beads and in the case of aerogels, the equivalent dry weight was placed in the tubes (0.013 g/L). The initial pH of the different solutions was not adjusted, resulting in a value of 5. The evolution of pH during the sorption process was monitored using a pH meter. Initial and pH solutions were determined by using a pH meter (Crison Digilab 517).

Results and discussion

Characterization of the CNFs, Alginate/CNF beads and CNF aerogels

The results of the characterization of the prepared CNFs is reflected in Table 1.

As it is possible to see, the obtained CNFs presented a carboxyl content of 1837 μeq·g/g. This indicates the high oxidation degree of cellulose, which led to a cationic demand of 2678 μeq·g/g. In fact, lower amounts of NaClO during TEMPO-mediated oxidation leads to CNFs with significantly lower carboxyl content, which at the same time, present lower physic and mechanical performance (Tarrés et al. 2017). However, for the proposed application, high oxidation

Table 1 Characterization of the obtained CNFs

Sample	CNF-TEMPO 25
Carboxyl content (μeq·g/g)	1837 ± 99
Cationic demand (μeq·g/g)	2678 ± 201
Specific surface (m²/g)	409
Diameter (nm)	6,5
Transmittance at 800 nm (%)	98.1 ± 1.2
Yield of fibrillation (%)	97.8 ± 0.9
WRV (g H₂O/g)	16.3 ± 1.1
DP (−)	203 ± 2
Length* (nm)	113
Aspect ratio	17.4

degrees are required if the highest performance of the columns wants to be achieved, since the presence of COOH and COONa groups will promote the adsorption of Cu^{2+} cations in the CNF surface (Fiol et al. 2004). Considering the mathematical models from the previous section, these values allowed to estimate the specific surface and the diameter, obtaining values of 409 m²/g and 6.5 nm, respectively. In fact, taking into account the obtained cationic demand, the yield of fibrillation of 97.8% was completely expected, which was later corroborated by the transmittance at 800 nm of wavelength (98.1%). The main reason behind applying such high oxidation degree was to have as much free carboxyl groups (either in acidic or salt form) at the surface of the cellulose chains to further improve the retention of divalent ions. In addition, high specific surface CNFs can lead to more porous structures when freeze-dried, meaning that the available surface to adsorb substances can be higher as well. The water retention capacity of the obtained

CNFs accounted for 16.3 g of chemically bonded water per g of CNFs, indicating the huge hydrophilic character thereof. This high water retention capacity can be expected to become a drawback for water depuration applications, since water flow could be hindered, dramatically decreasing the efficiency of the columns and, thus, making imperative the partial modification of the character of CNFs. According to the linear regression reported by Shinoda et al. (2012), the DP of TEMPO-oxidized CNFs can be correlated to the length of the CNFs. Taking into account this linear behavior, the average length of the CNFs was calculated to be 113 nm, leading to an aspect ratio (length/diameter) of 17.4. Taking into account that CNFs contain several amorphous domains, this aspect ratio should promote the entanglement thereof, exhibiting flexibility when they are properly processed to create aerogels. In addition, in the case of Alginate/CNFs beads, the aspect ratio will promote the entanglement inside the alginate matrix, being, in principle, beneficial for the dimensional stability thereof.

The Alginate/CNF beads were characterized, as reflected in Table 2, in terms of water content, density and diameter.

Apparently, the incorporation of moderate amounts of CNFs had no effect on water content, which accounted for about 95% in all cases. Surprisingly, the density of the beads was decreased from 0.9533 to 0.7513 g/mL with the incorporation of 0.2 wt% of CNFs. Then, as the amount of CNFs was increased, density was also enhanced. Since the water content is about 95% in all cases, no significant differences on beads density was expected as the amount of CNFs was increased. Nonetheless, something surprising was the shape and size of the beads containing CNFs. Taking into account that the micropipette tip was the same for all the experimental batch, the diameter of the beads was significantly higher when CNFs were used. In addition, their diameter were found to be higher with increasing amounts of CNFs. This behavior is completely understandable considering the huge anionic character of CNFs. The repulsive forces that COO^- groups impart within the bead significantly increased the volume thereof. This fact could explain the initial decrease on beads density. Although the density of cellulose has been extensively reported to be approximately 1.5 g/cm^3 (Delgado-Aguilar et al. 2015) and, in principle, any bead containing CNFs should be denser than those prepared only with alginate, the increase on the whole volume is palliating this effect. In fact, there is a perfect correlation between the bead diameter and the CNF content, described by a second order polynomial equation. The amount of CNFs was limited to 0.8 wt% due to limitations on the viscosity of the CNFs suspension.

As described in the previous section, CNF-based aerogels were prepared and characterized. In principle, the high specific surface of nanocellulose-based aerogels should promote the adsorption of the heavy metals on the CNF surface. This adsorption should be conducted by means of ionic exchange since, depending on the pH, the surface of the CNFs will present COOH or COONa groups (Fujisawa et al. 2011). In fact, aerogels are three dimensional structures built up of a network of thousands of CNFs, which confer them a huge porosity and, thus, promotes the water flow, while ions can be retained at the surface. In order to further understand how CNFs are structured in an aerogel, FE-SEM images were taken (Fig. 2).

As detailed in the previous section, the consistency of the CNF suspension was set at 0.5 wt%. At such consistency, TEMPO-oxidized CNFs are still in the form of gel, meaning that they are distributed along the suspension, creating a 3D network. Then, the suspension was frozen and then dried by means of water sublimation, leading to the abovementioned network but in its dry form. In this sense, several pores were created and, thus, the specific surface of the device was significantly high. Such structure can be observed in Fig. 2.

Table 2 Physical characterization of the Alginate/CNF beads

Sample	Water content (%)	Bead density (g/mL)	Bead diameter (mm)
Alginate/CNF_0.2	94.83 ± 0.20	0.7513 ± 0.05	3.00 ± 0.17
Alginate/CNF_0.5	96.37 ± 0.04	0.9291 ± 0.01	3.56 ± 0.07
Alginate/CNF_0.8	95.34 ± 0.18	1.0601 ± 0.05	3.72 ± 0.42
Alginate	95.35 ± 2.20	0.9533 ± 0.03	2.44 ± 0.03
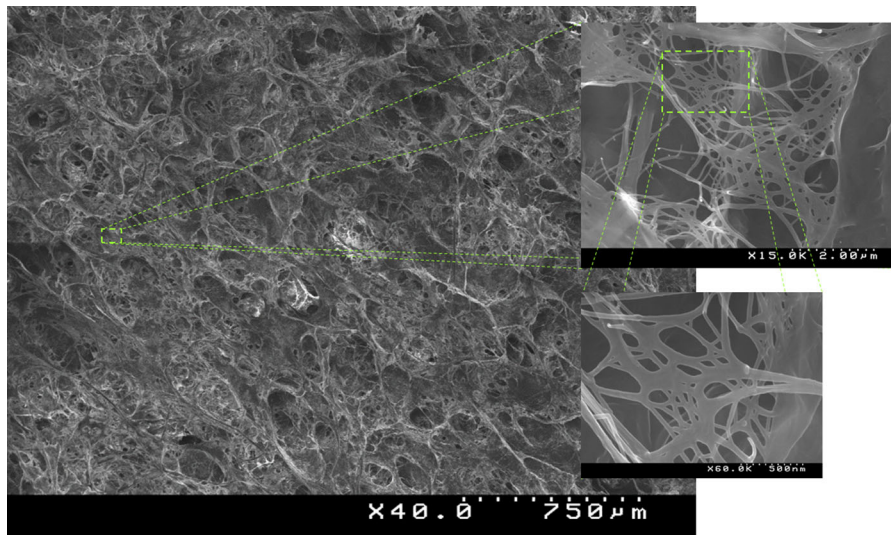
Fig. 2 FE-SEM images from the CNF-based aerogels at different magnification

Cu(II) uptake: batch procedure

Figure 3 shows the amount of cooper removed from the Cu(II) solutions at different concentration when alginate beads with different CNF content were used.

Apparently, there is no direct influence on copper removal as the amount of CNFs into the alginate-based beads increases. Indeed, this behavior was observed regardless the Cu^{2+} concentration of the solutions. The pure alginate beads adsorbed about 60.42, 35.84 and 20.38% of Cu^{2+} from the 15, 100 and 1000 mg/L solutions. Taking into account these adsorption rates, it is clear that the adsorption capacity of CFN in beads

is quite limited. In fact, considering that 15 mL of each solution were incorporated to 35 beads per batch, the amount of adsorbed Cu^{2+} per bead was higher as the copper concentration increased. In addition, considering the density of the beads, their volume and water content, the amount of Cu^{2+} per dry gram can be calculated, as reflected in Table 3.

The initial pH of the solution ranged from 4.6 to 5.7 for the highest (1500 mg/L) and the lowest (15 mg/L) copper concentration, respectively. After the sorption process, the pH experienced a slight decrease (0.2 pH units) in all experiments, indicating that some protons were released from the sorbent to the solution. This

Fig. 3 Cu(II) removal by CNF beads as a function of CNF content in beads. Discontinuous lines represent the pure alginate beads (0% CNFs)
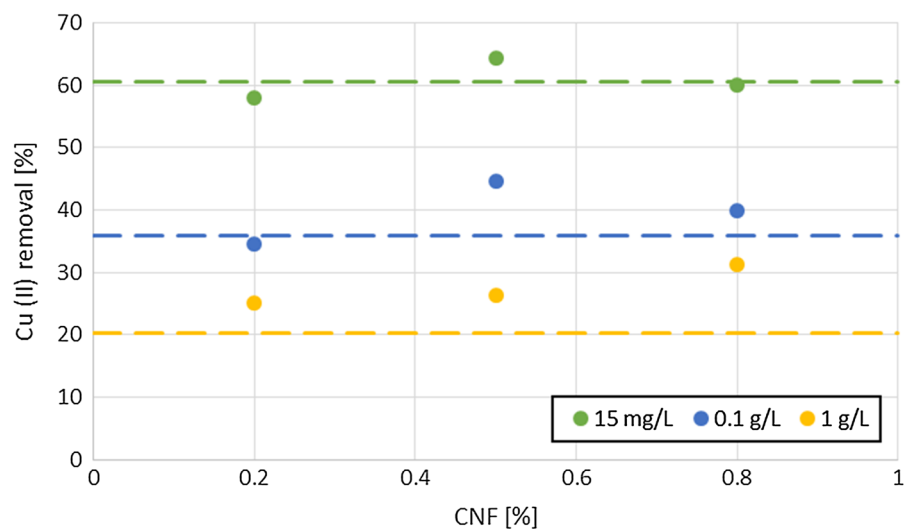
Table 3 Specific Cu^{2+} adsorption of the pure and CNF-containing alginate beads

| Cu^{2+} concentration (mg/L)	Sample	Cu^{2+} removal (%)	Cu^{2+} adsorbed (μg/bead)	q_e (mg/g)
15	Alginate	60.42	3.88	11.52
	Alginate/CNF_0.2	57.85	3.72	6.77
	Alginate/CNF_0.5	64.31	4.13	5.19
	Alginate/CNF_0.8	60.08	3.86	2.90
100	Alginate	35.84	15.36	45.56
	Alginate/CNF_0.2	34.56	14.81	26.97
	Alginate/CNF_0.5	44.67	19.14	24.03
	Alginate/CNF_0.8	39.97	17.13	12.86
1000	Alginate	20.38	87.34	259.05
	Alginate/CNF_0.2	25.11	107.61	195.98
	Alginate/CNF_0.5	26.36	112.97	141.79
	Alginate/CNF_0.8	31.28	134.06	100.68

q_e: Cu(II) adsorbed per gram of adsorbent (mg/g)

release could be originated by the presence of carboxylic acids at the surface of CNFs, which are highly oxidized. Considering the removal of Cu^{2+} in relative terms and taking as reference the initial concentration of the different solutions, no clear tendencies were found. In fact, despite the initial Cu^{2+} concentration, the removal capacity varied regardless the amount of CNFs. However, considering that the amount of dry alginate and CNFs that each bead contained, a clear tendency can be observed. In all cases, the amount of Cu^{2+} adsorbed per dry gram decreased following a second order polynomial expression, indicating that the presence of CNFs hinders the adsorption of the heavy metal. Here, there are several effects that might be influencing the ionic exchange capacity of the beads. On the one hand, the greater water retention capacity of CNFs against alginate can hinder the ionic exchange between Cu^{2+} cations and the COONa and COOH groups from cellulose surface. In fact, as the amount of CNFs was increased, the diameter of the beads was also increased, indicating that the penetration of the Cu^{2+} suspension became more difficult. On the other, the alginate was encapsulating such CNFs and, at the same time, several interactions between alginate and CNFs may occur, such as Van der Waals forces, hydrogen bonding and also ionic exchange between the Ca^{2+} cations from alginate and Na^+ and H^+, from the CNF surfaces, creating a kind of ionic crosslinking between

the two phases of the beads. In fact, the ionic interaction between carboxyl groups (either in its acidic or salt form) with heavy metals has been previously studied and discussed in the case of alginate beads and it is reported that Cu^{2+} and Ca^{2+} cations will be exchanged, being this the main mechanism involved in the adsorption (Jodra and Mijangos 2001; Veglio et al. 2002; Fiol et al. 2006). Indeed, according to Batmaz et al. (2014), the presence of ions inside the beads can increase the ionic strength of the solution, considering as solution the content of the beads. In this sense, as the amount of CNFs was increased inside the beads, the amount of carboxylate groups was increased as well inside the beads. In this sense, the large number of charged Na^+ and H^+ ions were competing with the Cu^{2+} molecules, hindering thus the interaction of the COO^- groups with the cations of the metal (Maurya et al. 2006).

For all the above, and taking into account that water inside the beads was probably hindering the interaction of the adsorbent with the Cu^{2+} molecules, the use of completely dried structures with high porosity and specific surface was proposed (Fig. 4).

According to a recent review (Hokkanen et al. 2016), there is a wide spectrum of modifications of cellulose to improve its performance as adsorbent of heavy metals. Among them, Klemm et al. (1998) reported that grafting different functional groups such as carboxyl, amine, amidoxime, nitrile and GME-

Fig. 4 Cu(II) removal with aerogels and alginate beads
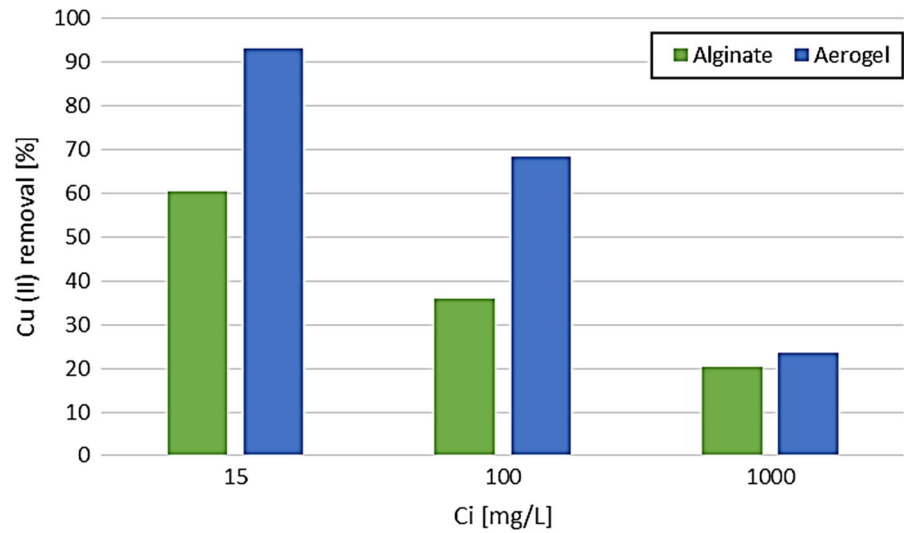
imidazole to cellulose could significantly improve the selectiveness of such cellulose-based adsorbents. Although the multiple ways of grafting different functional groups on cellulose, in this work carboxyl groups have been selected to act as binding groups due to the production process of CNFs, which originally increases the carboxyl content. As it is possible to see, at low adsorbate concentrations the difference between CNFs and alginate becomes more apparent. As this amount is increased, this difference becomes lower, being of the same magnitude when much charged solutions are used (1 g/L). Taking into account that the amount of CNFs was set as the equivalent dry weight to 35 alginate spheres, the specific adsorption can be calculated for each test (Table 4).

As it is possible to see, the aerogels adsorbed a higher amount of Cu^{2+} than the alginate beads. In fact,

there are two mechanisms that are probably promoting the higher adsorption on CNF surface: (i) on the one hand, the presence of highly charged water with Ca^{2+} cations may hinder the interaction of the COO^- groups with the Cu^{2+} cations; (ii) on the other, the higher specific surface of the CNF-based aerogels should increase the availability of COO^- groups where to retain the Cu^{2+} cations. Considering these two factors, the adsorption capacity of the aerogels should be even higher. Nonetheless, while drying, the hornification phenomena probably decreased such COO^- groups availability (Hubbe 2007). In this sense, in principle, dosing the CNFs in its wet state should be the best option, but their recovery would become difficult and expensive.

Table 4 Specific Cu^{2+} adsorption of the alginate beads and CNF-based aerogel

Cu^{2+} concentration (mg/L)	Sample	Cu^{2+} removal (%)	Cu^{2+} adsorbed (μg/bead)	q_e (mg/g)
15	Alginate	60.42	0.11	11.52
	Aerogel	93.33	0.17	17.79
100	Alginate	35.84	0.44	45.56
	Aerogel	68.47	0.84	87.03
1000	Alginate	20.38	2.50	259.05
	Aerogel	23.65	2.90	300.61

q_e: Cu^{2+} adsorbed per gram of adsorbent (mg/g)

Adsorption isotherms

The Langmuir isotherm can be described by the mathematical expression reflected in Eq. 7 (Hsi and Langmuir 1985; Bhatnagar and Jain 2005; Mall et al. 2005):

$$q_e = \frac{q_m K_a C_e}{1 + K_a C_e} \qquad (7)$$

where q_m is the maximum amount of Cu(II) that can be adsorbed per gram of adsorbent (mg/g) in equilibrium, Ce is the equilibrium concentration of free Cu(II) molecules in the solution (mg/L), K_a is a constant related to the energy of adsorption (L/mg), which reflects the affinity between the metal and the adsorbent. In fact, the values of K_a and q_m can be extracted by means of rearranging the isotherm above the its linearized form (Eq. 8).

$$\frac{1}{q_e} = \frac{1}{K_a q_m C_e} + \frac{1}{q_m} \qquad (8)$$

Thus, plotting $1/q_e$ as a function of $1/C_e$, where $1/K_a q_m$ is the slope and $1/q_m$, the intercept, a value for K_a and q_m can be found. Table 5 shows the output data from the linear regression of the Langmuir isotherm for each adsorbent and the isotherms can be observed in Figure S1. In all cases, the correlation was between 0.96 and 0.99, indicating that the obtained data can be described by the Langmuir isotherm.

In the case of alginate-based beads, the maximum adsorption capacity (q_m) decreased as the amount of CNFs was increased, as it has been discussed before. However, when aerogels were used, the adsorption capacity was increased in a 33.44% with regard to the alginate beads. In addition, in terms of affinity (K_a) between Cu^{2+} and CNFs, it was found that it was about 7 times higher than between Cu^{2+} and alginate.

Table 5 Langmuir isotherm parameters for Cu(II) sorption onto CNF beads and aerogel

$T = 20 \pm 1$ °C	q_m (mg/g)	K_a (L/mg)	R^2
Alginate	263.1	0.0186	0.959
Alginate/CNF_0.2	204.1	0.0162	0.978
Alginate/CNF_0.5	142.8	0.0153	0.968
Alginate/CNF_0.8	105.2	0.0095	0.969
Aerogel	303.0	0.1310	0.996

In fact, comparing the obtained results with some others available in the literature related to the effect of carboxyl groups on cellulose surface, and taking into account that 1 mmol of Cu^{2+} corresponds to 63.55 mg, the following comparison can be performed (Fig. 5).

Alginate beads showed better performance than microfibrillated cellulose modified with succinic anhydride, wood pulp modified with citric acid and cellulose nanocrystals. In addition, as it has been previously discussed, as the amount of CNFs was increased in the alginate beads, the adsorption capacity was significantly decreased due to the increase on the ionic strength inside the beads. In fact, the q_m of alginate beads containing 0.5 and 0.8 wt% of CNFs were of the same magnitude than microfibrillated cellulose with succinic acid and cellulose nanocrystals, indicating that the presence of carboxyl groups on their surface should be approximately the same. When aerogels were used, such adsorption capacity was raised to 4.77 mmol/g, indicating the higher Cu^{2+} adsorption capacity. Something surprising is that Hokkanen et al. (2013) found a value of K_a for such adsorbent and Cu^{2+} of 58.9 L/mmol, being a value significantly higher than the value found in the present work, which accounted for 0.1310 L/mg in the case of aerogels which is equivalent to 8.33 L/mmol. Nonetheless, the value they found for such adsorption was not adjusted to a Langmuir isotherm, since the linear regression exhibited a R^2 of 0.849. Low et al. (2004) adopted a strategy based on wood pulp also modified with succinic anhydride, obtaining a maximum Cu^{2+} adsorption capacity of 0.37 mmols/g. The main difference between using microfibrillated cellulose and wood pulp is the specific surface. While the strategy adopted by Hokkanen et al. (2013) promotes the interaction between the Cu^{2+} cations with the surface of the modified cellulose chains, in the work presented by Low et al. (2004) the availability of COO^- groups was significantly lower. In fact, this effect was also observed in the work of Alves-Gurgel et al. (2008), since the adsorption capacity was of the same magnitude. In fact, assuming that specific surface has a predominant role on Cu^{2+} adsorption, the obtained q_m by Batmaz et al. (2014) is completely understandable, although the work was carried out with dyes, since COO^- groups were introduced onto cellulose nanocrystals (CNCs) by means of TEMPO-mediated oxidation, the same treatment than in the
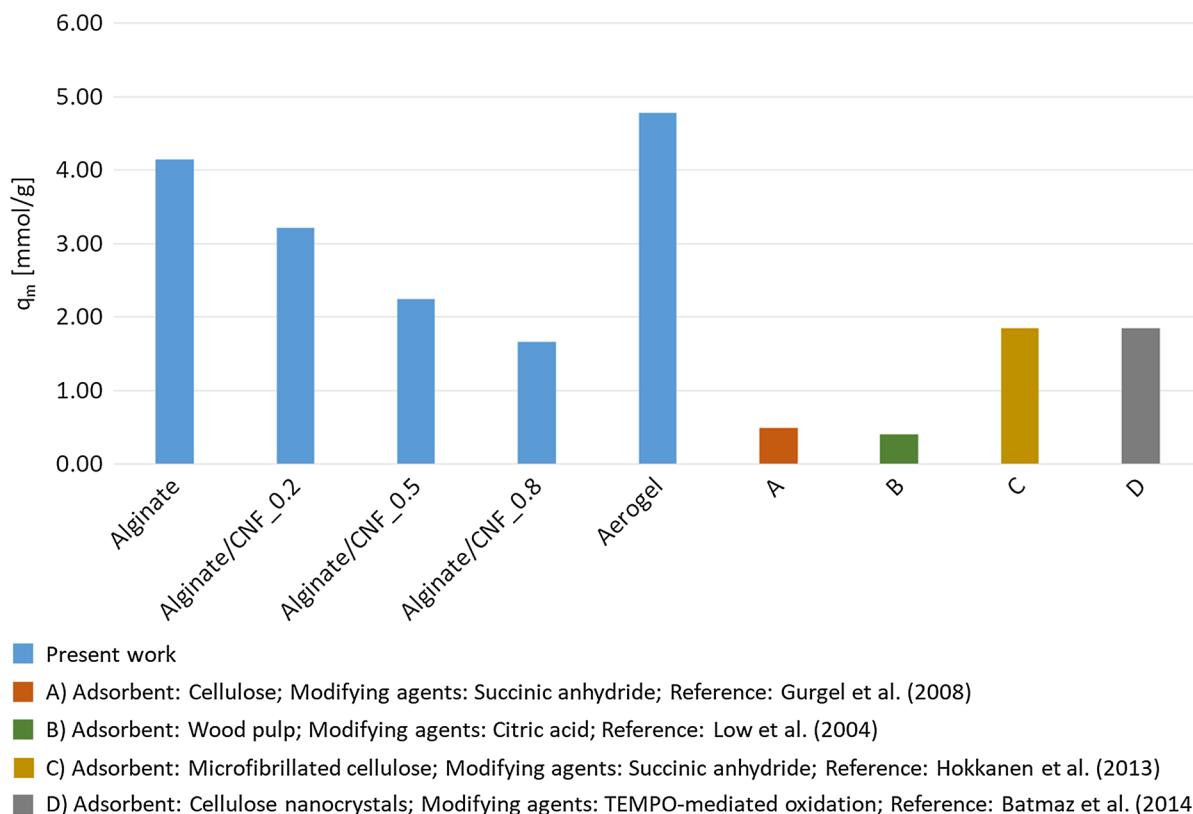
Fig. 5 Maximum Cu^{2+} adsorption capacity of different alginate and cellulose-based adsorbents

present work. Nonetheless, the lower capacity of CNCs to create entangled networks versus CNF has a direct impact on the adsorption capacity and the affinity between the adsorbate and the adsorbent (lower K_a values), making the difference between both systems more apparent, either in Cu^{2+} adsorption or dye adsorption.

Another important aspect in the design of heavy metals adsorbents is the regeneration capacity thereof. For this, Mall et al. (2005) described the R_L factor, which is dimensionless, that is commonly used to describe the favorability and feasibility of the adsorption process (Eq. 9).

$$R_L = \frac{1}{1 + K_a C_i} \qquad (9)$$

where C_i is the initial Cu^{2+} concentration in solution (mg/L) and K_a is the Langmuir constant (L/mg). The isotherm can be considered as favorable if R_L is comprised between 0 and 1, unfavorable if it is higher than 1, linear if it is equal to 1 and irreversible if it equals to 0. In all cases, values between 0 and 1 were

found, being the aerogel the one that presented closer values to 0. In this sense, although the adsorption capacity of the fully CNF-based device was the highest, the regeneration thereof, in principle, will be more challenging. Results can be observed in Table S1.

Conclusions

In this work, two different ways of using TEMPO-oxidized CNFs for Cu(II) removal have been approached. On the one hand, CNF entrapment into calcium alginate beads and, on the other, the development of 3D porous CNF-based structures. In the case of the calcium alginate beads, it was found that the presence of CNFs hindered the adsorption of Cu^{2+} ions mainly due to the increasing number of inner ions competing with the metal ions. In this sense, it appears that the ionic strength inside the spheres increased with increasing amounts of COO– groups (CNF/alginate ratio), hindering the entrapment of Cu^{2+}

inside the beads. Indeed, the maximum adsorption capacity was decreased as the amount of CNFs was increased.

The 3D-structured aerogels resulted in permeable and porous structures suitable to be used as sorbent materials to remove contaminants from aqueous solutions. In this sense, the maximum adsorption capacity of CNF-based aerogels was significantly higher than in the case of neat calcium alginate beads.

Although the presence of CNFs in alginate beads was found to be not beneficial in terms of Cu(II) removal, both systems could be described by Langmuir isotherm model in the studied concentration range of copper(II) ions, confirming that the copper sorption was a favorable process. In addition, the obtained data was comparable to the existing literature, being significantly better in some cases where carboxylated cellulose is used.

Overall, TEMPO-oxidized CNFs have been found to be a potential candidate for wastewater treatment, especially in their freeze-dried form and in batch. However, continuous experiments must be performed in the future to further explore the opportunities of CNFs in wastewater treatment, especially in their aerogel form, since it is clear that their presence inside the beads is not beneficial at all.

References

Alves-Gurgel LV, Karnitz-Junior O, de Freitas-Gil RP, Gil LF (2008) Adsorption of Cu(II), Cd(II), and Pb(II) from aqueous single metal solutions by cellulose and mercerized cellulose chemically modified with succinic anhydride. Bioresour Technol 99:3077–3083. https://doi.org/10.1016/j.biortech.2007.05.072

Batmaz R, Mohammed N, Zaman M et al (2014) Cellulose nanocrystals as promising adsorbents for the removal of cationic dyes. Cellulose 21:1655–1665. https://doi.org/10.1007/s10570-014-0168-8

Besbes I, Alila S, Boufi S (2011) Nanofibrillated cellulose from TEMPO-oxidized eucalyptus fibres: effect of the carboxyl content. Carbohydr Polym 84:975–983. https://doi.org/10.1016/j.carbpol.2010.12.052

Bezbaruah AN, Krajangpan S, Chisholm BJ et al (2009) Entrapment of iron nanoparticles in calcium alginate beads for groundwater remediation applications. J Hazard Mater 166:1339–1343. https://doi.org/10.1016/j.jhazmat.2008.12.054

Bhatnagar A, Jain AK (2005) A comparative adsorption study with different industrial wastes as adsorbents for the removal of cationic dyes from water. J Colloid Interface Sci 281:49–55. https://doi.org/10.1016/j.jcis.2004.08.076

Delgado-Aguilar M, González I, Pèlach MA et al (2015) Improvement of deinked old newspaper/old magazine pulp suspensions by means of nanofibrillated cellulose addition. Cellulose 22:789–802. https://doi.org/10.1007/s10570-014-0473-2

Espinosa E, Tarrés Q, Delgado-Aguilar M et al (2016) Suitability of wheat straw semichemical pulp for the fabrication of lignocellulosic nanofibres and their application to papermaking slurries. Cellulose 23:837–852. https://doi.org/10.1007/s10570-015-0807-8

Fiol N, Poch J, Villaescusa I (2004) Chromium(VI) uptake by grape stalks wastes encapsulated in calcium alginate beads: equilibrium and kinetics studies. Chem Speciat Bioavailab 16:25–33. https://doi.org/10.3184/095422904782775153

Fiol N, Escudero C, Poch J, Villaescusa I (2006) Preliminary studies on Cr(VI) removal from aqueous solution using grape stalk wastes encapsulated in calcium alginate beads in a packed bed up-flow column. React Funct Polym 66:795–807. https://doi.org/10.1016/j.reactfunctpolym.2005.11.006

Fujisawa S, Okita Y, Fukuzumi H et al (2011) Preparation and characterization of TEMPO-oxidized cellulose nanofibril films with free carboxyl groups. Carbohydr Polym 84:579–583. https://doi.org/10.1016/j.carbpol.2010.12.029

Glover-Kerkvliet J (1995) Environmental assault on immunity. Environ Health Perspect 103:236–239. https://doi.org/10.1289/ehp.95103236

Henriksson M, Henriksson G, Berglund LA, Lindström T (2007) An environmentally friendly method for enzyme-assisted preparation of microfibrillated cellulose (MFC) nanofibers. Eur Polym J 43:3434–3441. https://doi.org/10.1016/j.eurpolymj.2007.05.038

Hii C, Gregersen Ø, Chinga-Carrasco G, Eriksen Ø (2012) The effect of MFC on the pressability and paper properties of TMP and GCC based sheets. Nord Pulp Pap Res J 27:388–396. https://doi.org/10.3183/NPPRJ-2012-27-02-p388-396

Hokkanen S, Repo E, Sillanpää M (2013) Removal of heavy metals from aqueous solutions by succinic anhydride modified mercerized nanocellulose. Chem Eng J 223:40–47. https://doi.org/10.1016/j.cej.2013.02.054

Hokkanen S, Bhatnagar A, Sillanpää M (2016) A review on modification methods to cellulose-based adsorbents to improve adsorption capacity. Water Res 91:156–173. https://doi.org/10.1016/j.watres.2016.01.008

Hsi C-KD, Langmuir D (1985) Adsorption of uranyl onto ferric oxhydroxides: application of the surface complexation site-binding model. Geochim Cosmochim Acta 49:1931–1941

Hubbe MA (2007) Paper's resistance to wetting: a review of internal sizing chemicals and their effects. BioResources 2:106–145. https://doi.org/10.15376/biores.2.1.106-145

Isogai A, Saito T, Fukuzumi H (2011) TEMPO-oxidized cellulose nanofibers. Nanoscale 3:71–85. https://doi.org/10.1039/c0nr00583e

Jodra Y, Mijangos F (2001) Ion exchange selectivities of calcium alginate gels for heavy metals. Water Sci Technol 43:237–244. https://doi.org/10.2166/wst.2001.0095

Klemm D, Philipp B, Heinze T, Heinze U (1998) Comprehensive cellulose chemistry, vol 1. Wiley-VCH, Weinheim

Lay M, Méndez JA, Delgado-Aguilar M et al (2016) Strong and electrically conductive nanopaper from cellulose nanofibers and polypyrrole. Carbohydr Polym. https://doi.org/10.1016/j.carbpol.2016.06.102

Lin N, Dufresne A (2014) Nanocellulose in biomedicine: current status and future prospect. Eur Polym J 59:302–325. https://doi.org/10.1016/j.eurpolymj.2014.07.025

Lizundia E, Delgado-Aguilar M, Mutjé P et al (2016) Cu-coated cellulose nanopaper for green and low-cost electronics. Cellulose 23:1997–2010. https://doi.org/10.1007/s10570-016-0920-3

Low KS, Lee CK, Mak SM (2004) Sorption of copper and lead by citric acid modified wood. Wood Sci Technol 38:629–640. https://doi.org/10.1007/s00226-003-0201-9

Maatar W, Boufi S (2015) Poly(methacylic acid-co-maleic acid) grafted nanofibrillated celluloseas a reusable novel heavy metal ions adsorbent. Carbohydr Polym 126:199–207

Mahfoudhi N, Boufi S (2017) Nanocellulose as a novel nanostructured adsorbent for environmental remediation: a review. Cellulose 24:1171–1197

Mall ID, Srivastava VC, Agarwal NK, Mishra IM (2005) Adsorptive removal of malachite green dye from aqueous solution by bagasse fly ash and activated carbon-kinetic study and equilibrium isotherm analyses. Colloids Surfaces A Physicochem Eng Asp 264:17–28. https://doi.org/10.1016/j.colsurfa.2005.03.027

Maurya NS, Mittal AK, Cornel P, Rother E (2006) Biosorption of dyes using dead macro fungi: effect of dye structure, ionic strength and pH. Bioresour Technol 97:512–521. https://doi.org/10.1016/j.biortech.2005.02.045

Pidwirny M (2006) The hydrologic cycle. In: Fundamentals of physical geography, 2nd edn. http://www.physicalgeography.net/fundamentals/8b.html. Accessed 17 May 2018

Saito T, Kimura S, Nishiyama Y, Isogai A (2007) Cellulose nanofibers prepared by TEMPO-mediated oxidation of native cellulose. Biomacromol 8:2485–2491. https://doi.org/10.1021/bm0703970

Sehaqui H, Liu A, Zhou Q, Berglund LA (2010) Fast preparation procedure for large, flat cellulose and cellulose/inorganic nanopaper structures. Biomacromol 11:2195–2198. https://doi.org/10.1021/bm100490s

Serra A, González I, Oliver-Ortega H et al (2017) Reducing the amount of catalyst in TEMPO-oxidized cellulose nanofibers: effect on properties and cost. Polymers. https://doi.org/10.3390/polym9110557

Shinoda R, Saito T, Okita Y, Isogai A (2012) Relationship between length and degree of polymerization of TEMPO-oxidized cellulose nanofibrils. Biomacromol 13:842–849

Tarrés Q, Oliver-Ortega H, Llop M et al (2016) Effective and simple methodology to produce nanocellulose-based aerogels for selective oil removal. Cellulose 23:3077–3088. https://doi.org/10.1007/s10570-016-1017-8

Tarrés Q, Boufi S, Mutjé P, Delgado-Aguilar M (2017) Enzymatically hydrolyzed and TEMPO-oxidized cellulose nanofibers for the production of nanopapers: morphological, optical, thermal and mechanical properties. Cellulose. https://doi.org/10.1007/s10570-017-1394-7

Tarrés Q, Oliver-Ortega H, Ferreira PJ et al (2018) Towards a new generation of functional fiber-based packaging: cellulose nanofibers for improved barrier, mechanical and surface properties. Cellulose 25:683–695. https://doi.org/10.1007/s10570-017-1572-7

USGS (2013) The world's water. http://ga.water.usgs.gov/edu/earthwherewater.html. Accessed 17 May 2018

Veglio F, Esposito A, Reverberi AP (2002) Copper adsorption on calcium alginate beads: equilibrium pH- related models. Hydrometallurgy 65:43–57

Vinícius L, Gurgel A, Gil LF (2009) Adsorption of Cu(II), Cd(II), and Pb(II) from aqueous single metal solutions by succinylated mercerized cellulose modified with triethylenetetramine. Carbohydr Polym 77:142–149. https://doi.org/10.1016/j.carbpol.2008.12.014

Wan Ngah WS, Hanafiah MAKM (2008) Removal of heavy metal ions from wastewater by chemically modified plant wastes as adsorbents: a review. Bioresour Technol 99:3935–3948. https://doi.org/10.1016/j.biortech.2007.06.011

Zhang Z, Sèbe G, Rendtsch D et al (2014) Ultralightweight and flexible silylated nanocellulose sponges for the selective removal of oil from water. Chem Mater 26:2659–2668